

Processes going on in Nonfailed Rod during Accident Conditions (LOCA and RIA)

Volume II

Authors

Alfred Strasser

Aquarius Services, Sleepy Hollow, NY, USA

Friedrich Garzarolli

Fürth, Germany

Peter Rudling

ANT International, Skultuna, Sweden

Reviewed by

Charles Patterson

Clovis, CA, USA



A.N.T. INTERNATIONAL®

© September 2010

Advanced Nuclear Technology International

Krongjutarvägen 2C, SE-730 50 Skultuna

Sweden

info@antinternational.com

www.antinternational.com



Ecolabelled printed matter, 441 799

Disclaimer

The information presented in this report has been compiled and analysed by Advanced Nuclear Technology International Europe AB (ANT International®) and its subcontractors. ANT International has exercised due diligence in this work, but does not warrant the accuracy or completeness of the information.

ANT International does not assume any responsibility for any consequences as a result of the use of the information for any party, except a warranty for reasonable technical skill, which is limited to the amount paid for this assignment by each ZIRAT/IZNA programme member.

Foreword

Processes going on inside a nonfailed fuel rod may have dramatic impact on fuel performance during normal operation and during accident conditions such as Loss Of Coolant Accident (LOCA) and Reactivity Initiated Accident (RIA) as follows:

- Decrease in pellet density (and increase in pellet diameter) after some initial densification. The pellet diameter and the clad Inner Diameter (ID) determines the pellet-clad gap size which has a major impact on gap thermal conductivity (and fuel temperature) and Pellet Cladding Mechanical Interaction (PCMI) performance during a RIA event.
- The fuel melting temperature decreases slightly with exposure, due primarily to the accumulation of conversion and fission products and due to increasing oxygen potential.
- The formation of a high burnup rim zone at pellet average burnups in excess of about 50 MWd/kgU. Formation of this High Burnup Structure (HBS) is characterized by (or results from) a simultaneous formation of a sub-grain structure leading to an amorphous appearance, an increase in porosity and the transfer of fission gas from the HBS UO_2 matrix to the pores. The rim structure affects the thermal conductivity and is postulated to increase Fission Gas Release (FGR) during a RIA and LOCA due to fragmentation of the rim zone under the excessive overpressure in the pores.
- Thermal conductivity, density and heat capacity decrease with burnup and are addressed in most thermal-mechanical models that are structured for evaluations of fuel performance at moderate-to-high burnup. The thermal conductivity of UO_2 is a key parameter in fuel performance and in code calculations since conductivity impacts important properties such as fuel temperature, thermal expansion, FGR and gaseous swelling. Thermal conductivity is the product of thermal diffusivity, heat capacity, and density. The specific heat capacity and thermal conductivity of UO_2 are inter-related by way of density and thermal diffusivity. Heat capacity is a principal factor in the energy stored within a fuel rod and must be considered in LOCA and, RIA transient analyses.
- FGR – The release of the fission gases Xe and Kr in the UO_2 lattice to the rod void (plenum, pellet-cladding gap, etc.) will together with the rod void volume and gas temperature determine the fuel rod internal pressure. At a certain rod internal overpressure (compared to the system pressure), clad tensile stresses (due to the rod internal overpressure) above a critical value may cause reorientation the fuel clad hydrides from tangential to radial oriented. Radial hydrides may increase clad embrittlement and thereby reduce PCMI failure limit during a RIA event. Design limits ensure that hydride reorientation do not occur during normal operation.
- The Transient Fission Gas Release (TFGR) during and after a power ramp is also an area of interest. The TFGR value depends partly on the burnup, the fuel microstructure (e.g., grain size, porosity, etc.) and pellet-cladding mechanical interaction. The TFGR will increase cladding deformation during a RIA event. TFGR may also increase the risk of getting fuel dispersal (i.e., fuel particles leaves the fuel rod) during a LOCA and a RIA event. Fuel dispersal is considered a non-coolable geometry and is not accepted by regulators.

The objective of the Zirconium Alloy Technology (ZIRAT15) STR (Special Topic Report) Vol. I and II is to provide ZIRAT15 Members with the basic understanding of the processes occurring inside the fuel rod both during normal operation and accident conditions.

Volume I of the report describes the processes going on inside a nonfailed fuel rod during normal operation while Volume II of the report describes the corresponding information during accident conditions (RIA and LOCA).

The interested reader of the topics covered in this ZIRAT15 STR Vol. II is referred to the following references:

- Section on LOCA and RIA in the ZIRAT5-14/IZNA¹1-9 Annual Reports, ANT International, 2000-2009.
- ZIRAT9/IZNA4 STR on Loss of Coolant Accidents, LOCA, and Reactivity Initiated Accidents, RIA, in BWRs² and PWRs³ by Peter Rudling, Friedrich Garzarolli and Ron Adamson, ANT International, 2004.
- Nuclear fuel behaviour under reactivity-initiated accident (RIA) conditions, Nuclear Energy Agency (NEA) Report No. 6847, OECD, 2010.
- Nuclear fuel behaviour in Loss-of-coolant accident (LOCA) conditions, NEA Report No. 6846, OECD, 2009.
- Meyer R., *An assessment of fuel damage in postulated reactivity initiated accidents*, Nuclear Technology Vol. 155, 2006.
- Papin, Cazalis B., Frizonnet J. M., Desquines J., Lemoine F., Georgenthum V., Lamare F. and Petit M., *Summary and interpretation of the CABRI Rep-Na Program*, Nuclear Technology Vol. 157, 2007.

¹ Information on Zirconium Alloys

² Boiling Water Reactors

³ Pressurized Water Reactor

Contents

Foreword	II
1 RIA (Peter Rudling)	1-1
1.1 Introduction (Peter Rudling and Alfred Strasser)	1-1
1.2 Description of in-reactor and ex-reactor tests to simulate the RIA accident	1-5
1.2.1 Introduction	1-5
1.2.2 Pulse reactor characteristics	1-7
1.2.2.1 SPERT (USA)	1-7
1.2.2.2 PBF (USA)	1-7
1.2.2.3 IGR	1-7
1.2.2.4 BGR (Russia)	1-7
1.2.2.5 NSRR (Japan)	1-7
1.2.2.6 CABRI (France)	1-9
1.2.2.7 Summary of RIA tests	1-9
1.3 Clad failure mechanism	1-11
1.3.1 Introduction	1-11
1.3.2 Low burnup failures	1-13
1.3.3 High burnup failures	1-14
1.3.3.1 PCMI (low temperature failure)	1-14
1.3.3.1.1 Introduction (Friedrich Garzarolli)	1-14
1.3.3.1.2 Failure mechanism	1-15
1.3.3.1.2.1 Radial crack propagation	1-16
1.3.3.1.2.2 Axial crack propagation	1-16
1.3.3.1.3 Influence of clad tube design on PCMI failure mechanism	1-17
1.3.3.1.4 Influence of clad tube conditions on PCMI	1-17
1.3.3.1.4.1 Irradiation damage	1-17
1.3.3.1.4.2 Direct effects of clad oxide layer	1-18
1.3.3.1.4.3 Embrittlement effects of hydrides	1-19
1.3.3.1.5 Influence of temperature	1-24
1.3.3.1.6 Impact of loading condition	1-26
1.3.3.2 Ballooning and creep burst (HT failure)	1-27
1.3.4 Fuel dispersal (Friedrich Garzarolli and Peter Rudling)	1-30
1.3.4.1 Fuel-coolant interaction	1-31
1.4 Description of the various parameters impacting RIA fuel performance	1-34
1.4.1 Introduction	1-34
1.4.2 CZP and HZP	1-34
1.4.2.1 Introduction	1-34
1.4.2.2 Effect of coolant temperature (CZP, HZP)	1-35
1.4.2.2.1 Introduction	1-35
1.4.2.2.2 Effect on PCMI	1-36
1.4.3 Pulse characteristics (power increase rate, enthalpy increase, peak enthalpy, pulse width)	1-39
1.4.3.1 Introduction	1-39
1.4.3.2 Pulse width	1-40
1.4.3.2.1 Introduction	1-40
1.4.3.2.2 Effect of pulse width on PCMI failure tendency	1-41
1.4.3.2.3 Effects of pulse width on fuel dispersal tendency	1-43
1.4.3.3 Max fuel enthalpy increase	1-44
1.4.3.3.1 Introduction	1-44
1.4.3.3.2 Effects of enthalpy increase	1-45
1.4.3.3.2.1 Cladding deformation	1-45
1.4.3.3.2.2 TFGR	1-46
1.4.4 Fuel parameters	1-48
1.4.4.1 Burnup effects	1-48
1.4.4.1.1 Introduction	1-48
1.4.4.1.2 Pulse characteristics	1-50

1.4.4.1.3	Radial distribution of power	1-50
1.4.4.1.4	RIM zone development	1-51
1.4.4.1.5	Melting temperature	1-52
1.4.4.1.6	Thermal conductivity	1-52
1.4.4.1.7	FGR	1-53
1.4.4.1.7.1	TFGR in UO ₂ fuel (Friedrich Garzarolli)	1-54
1.4.4.1.7.2	TFGR of MOX fuel	1-56
1.4.4.1.8	Pellet-clad gap and bonding	1-62
1.4.4.1.9	Fuel pellet transient fragmentation and pellet swelling	1-65
1.4.4.1.10	Fuel dispersal in UO ₂ rods	1-66
1.4.4.2	Enrichment	1-66
1.4.5	Cladding parameters	1-67
1.4.5.1	Clad temperature during RIA (effects of cladding heat-up, melting, boiling crises and quenching)	1-67
1.4.5.2	Cladding transient deformation during RIA	1-71
1.5	Results of energy and failure distribution calculations	1-72
1.5.1	CREAs in PWRs	1-72
1.5.2	RDAs in BWRs	1-74
1.6	Licensing RIA criteria	1-76
1.6.1	Introduction	1-76
1.6.1.1	Current US regulations	1-76
1.6.1.2	Modifications being considered to US requirements	1-77
1.6.1.3	Non – US regulations	1-79
2	LOCA (Peter Rudling)	2-1
2.1	Introduction (Alfred Strasser and Peter Rudling)	2-1
2.2	Description of the various parameters impacting LOCA fuel performance	2-7
2.2.1	Introduction	2-7
2.2.2	FGR and TFGR during LOCA (for source term) (Friedrich Garzarolli)	2-7
2.2.2.1	Introduction	2-7
2.2.2.2	FGR during base irradiation	2-8
2.2.2.3	Formation of high burnup rime zone during base irradiation and TFGR during LOCA	2-9
2.2.3	Ballooning, fuel relocation and blockage	2-13
2.2.3.1	Ballooning	2-13
2.2.3.2	Fuel relocation	2-14
2.2.3.2.1	Introduction	2-14
2.2.3.2.2	Effects	2-16
2.2.3.3	Coolant blockage	2-19
2.2.4	Burst	2-20
2.2.4.1	Introduction	2-20
2.2.4.2	Effect of fuel clad temperature	2-22
2.2.4.3	Impact of heating rate on burst strain	2-26
2.2.4.4	Effect of fuel clad stress (due to overpressurisation)	2-28
2.2.4.5	Effect of pre-LOCA hydrogen clad content	2-29
2.2.5	Oxidation (ECR)	2-31
2.2.5.1	Introduction	2-31
2.2.5.2	Effect of PCT and time at PCT (e.g. runaway oxidation)	2-33
2.2.5.3	Effect of Zr source material and surface treatment	2-36
2.2.6	Rupture	2-39
2.2.6.1	Introduction	2-39
2.2.6.2	Effect of pre-LOCA hydrogen clad content (increase solubility of oxygen in prior beta-Zr phase) and total hydrogen content	2-40
2.2.6.3	Effect of PCT	2-43
2.2.6.4	Effect of fuel-clad bonding	2-44
2.2.6.5	Effect of quenching	2-45
2.2.6.6	Effect of stress (fuel rod restraint)	2-48
2.2.6.7	Effect of temperature (at rod loading)	2-50

2.3	Description of in-reactor and ex-reactor tests simulating LOCA	2-52
2.3.1	Out-of-reactor tests	2-52
2.3.1.1	JAERI	2-52
2.3.1.2	Korea Atomic Energy Research Institute (KAERI)	2-53
2.3.1.3	ANL	2-54
2.3.1.4	The Russian PARAMETR-M and TEFSAI-19 facilities	2-56
2.3.2	In-reactor tests	2-57
2.3.2.1	PHEBUS test	2-57
2.3.2.2	LOCA tests in the Halden reactor	2-58
2.4	Licensing LOCA criteria	2-62
2.4.1	10CFR100	2-62
2.4.2	10CFR50 (ECCS criteria)	2-64
3	References	3-1
	Nomenclature	3-1
	Unit conversion	3-3

1 RIA (Peter Rudling)

1.1 Introduction (Peter Rudling and Alfred Strasser)

Reactor kinetics – About 99.4% of all neutrons are born directly in fission (*prompt neutrons*), with a very short lifetime, about 0.1 msec. However, approximately 0.64% of the neutrons are delayed (*delayed neutrons*⁴) because they come from decay of fission products, where the average delay time is about 15 seconds.

In the steady state condition, just as many neutrons are produced by fission as are lost by absorption and leakage from the reactor in a given time. In such a system, the condition for *criticality*, i.e. for a self-sustaining fission chain to be possible, in the infinite system is that the effective multiplication factor, $k_{\text{eff}} = 1$ ⁵.

During normal reactor operation, *delayed neutrons* are necessary to maintain power so the response to *reactivity* change⁶ is relatively slow and possible to control. The k_{eff} must be kept below 1.006 to keep the delayed neutrons in play. If not, the reactor will be *prompt critical*⁷ and the time behaviour will be decided by the short lifetime of the prompt neutrons. Any increase of k_{eff} above 1.006 will give very fast power increases.

However, water reactors are designed so that a power increase will generate negative *reactivity* feedback where a fuel temperature increase gives a fast negative feedback (Doppler effect). On the other hand, an increase in the moderator temperature and steam (void) fraction, gives a slower negative feedback. A slow reactivity increase may not cause any harm even if it is larger than 0.006 because of the negative feedback mechanisms.

Thus, the conditions for a reactor power transient like RIA to be of a concern are:

- It must be very fast.
- The reactivity added must be larger than 0.006.

Even a very fast transient will be stopped within fractions of a second by the fast negative feedback from the fuel temperature increase. Assisted by the slower moderator feedback the reactor protection system will then shut down the reactor.

RIA power pulse characteristics- The reactivity transient during a RIA results in a rapid increase in fuel rod power leading to a nearly adiabatic heating of the fuel pellets. The radial average peak fuel enthalpy is less than the associated radial average total energy deposition due to fuel to coolant heat transfer during the transient and also since a significant part of the total energy is due to delayed fission (Figure 1-1).

⁴ If β represents the fraction of the fission neutrons that are delayed, then $(1 - \beta)$ represents the prompt-neutron fraction.

⁵ $k_{\text{eff}} = \text{Rate of neutron production} / (\text{Rate of neutron absorption} + \text{Rate of neutron leakage})$.

⁶ The fractional departure of a system from criticality is often expressed by the reactivity, ρ , and defined by:

$$\rho \equiv \frac{k_{\text{eff}} - 1}{k_{\text{eff}}}.$$

⁷ When a reactor is critical on prompt neutrons alone, it is said to be prompt critical. It can be shown that a reactor becomes prompt critical when $\rho = \beta$ i.e., when the reactivity is equal to the fraction of delayed neutrons. A thermal reactor in which the fissile material is uranium-235 becomes prompt critical when

$\rho = 0.0065$, so that $k_{\text{eff}} = \frac{1}{1 - \rho}$ is then close to 1.0065. The prompt critical condition is sometimes used as

the basis for the reactivity unit dollar (\$) which is defined as *Reactivity in dollars* $\equiv \frac{\rho}{\beta}$. When a reactor is prompt critical, the reactor has a reactivity of exactly one dollar.

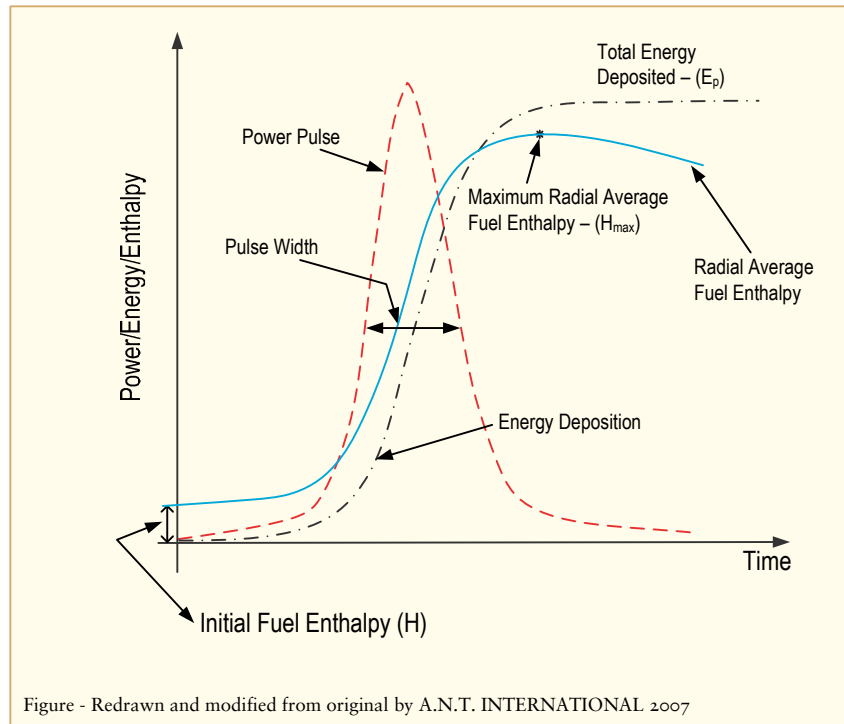


Figure 1-1: RIA power pulse characteristics [Montgomery et al, 2003].

The characteristics of the power pulse depend on the accident scenario – most importantly the *reactivity worth* of the ejected control rod⁸, but also on the core and fuel design, reactor operating state, and the time at which the accident occurs during the fuel cycle [Stelletta & Waeckel, 1997] (Figure 1-54). The reactivity worth of the ejected control rod depends on its position and insertion depth in the core, the core axial power shape and the fuel burnup distribution close to the ejected rod. The local value for the pulse amplitude, P_{\max} , depends on fuel burnup, core loading pattern, the distance from the ejected control rod, and the reactivity worth of the ejected rod. The same is true for the local fuel enthalpy. The, P_{\max} , falls off with increasing distance from the ejected control rod, and it also depends on fuel burnup.

RIA design basis accidents – The design basis RIA in a PWR is the Control Rod Ejection Accident (CREA) and in a BWR the control Rod Drop Accident (RDA). The CREA is based on the assumption of a mechanical failure of the control rod drive mechanism located on the reactor vessel top, followed by the ejection of the mechanism and the control rod by the internal reactor pressure. The BWR RDA is assumed to occur if a control rod is detached from its drive mechanism in the core bottom, stays stuck while inserted in the core, then if loosened, drops out of the core by gravity, without involvement of a change in reactor pressure as in the CREA. As a result, the BWR power pulses are slower and the pulse widths wider than for a PWR. Since the rod worth decreases with increased power level and with a decrease in control rod insertion within the core, Hot Zero Power HZP should be the most limiting initial condition for the CREA, see also Section 1.4.2. With respect to reactivity addition, the most severe RDA would occur at Cold Zero Power (CZP) conditions, i.e. at a state with the coolant close to Room Temperature (RT) and atmospheric pressure, and the reactor at nearly zero power [Agee et al, 1995] and [Nakajima et al, 2002]. The degree of reactivity addition during RDA is strongly affected by the coolant subcooling, since vapour generation effectively limits the power transient.

⁸ The change in reactivity it can produce by changing its axial position in the core.

Contrary to PWRs/BWRs, Canadian Deuterium Uranium (CANDU) reactors have a positive coolant void reactivity coefficient [Snell et al, 1990]. Thus, coolant boiling, e.g. due to:

- Inadvertent heating of the feedwater or,
- a reduction of coolant flow,
- results in a reactivity increase in CANDU reactors [Luxat & Spencer, 1988].

A guillotine break of a large diameter header to a loop of the heat transport system (LOCAs) is one of the most severe postulated scenarios with respect to reactivity insertion rate resulting in a potential core average power increase of 3-4 times of its nominal value. The power surge is terminated by the shutoff system, and the pulse width is about 1 s [Jeong & Suk, 2006].

RIA fuel performance – In a fresh fuel rod, the fissile material consists predominantly of ^{235}U , which is usually uniformly distributed in the fuel pellets. Hence, both power and fission products are generated with a relatively small variation along the fuel pellet radius. However, with increasing burnup, there is a non-uniform buildup of fissile plutonium isotopes through neutron capture by ^{238}U and formation of ^{239}Pu and heavier fissile isotopes of plutonium. Since the neutron capture takes place mainly at the pellet surface, the distributions of fissile material, fission rate and fission products will develop marked peaks at the pellet surface as fuel burnup increases. The shapes of these distributions are dependent not only on irradiation time, but also on the fuel initial content of ^{235}U , pellet radius and the neutron energy spectrum of the reactor. Figure 1-2 shows an example of the radial fuel temperature distribution for an intermediate/high burnup fuel rod and it is clear that the highest RIA temperatures are occurring at the fuel pellet periphery. The impact of various RIA parameters on fuel performance is discussed in Section 1.4.

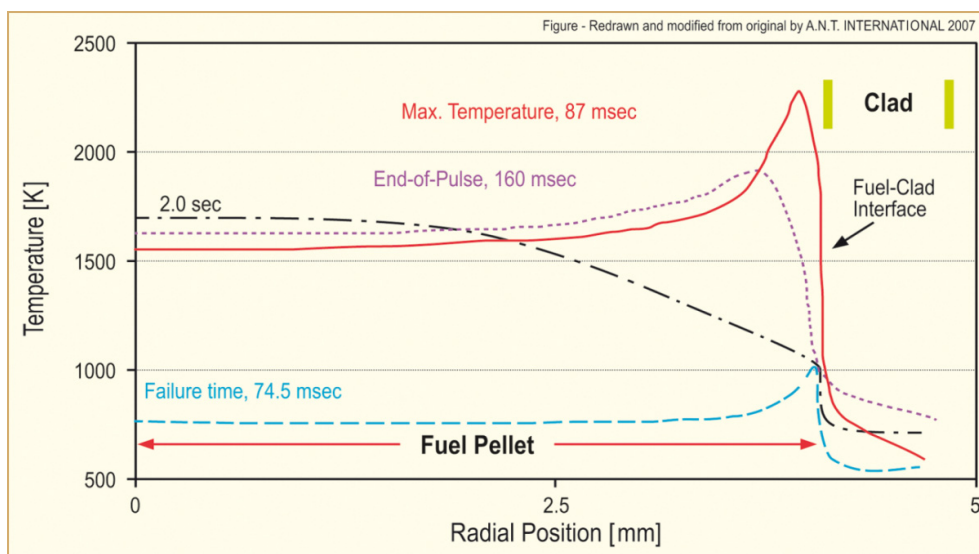


Figure 1-2: Calculations of the fuel radial temperature in the CABRI REP Na-1 test (Burnup 65 MWd/kgU and pulse width 9.5 ms) modified figure according to [Montgomery & Rashid, 1997].

Fuel failure modes – There are different possible failures modes for the fuel, the details of which are described in Section 1.3.

At low burnup fuel cladding failures may occur due to:

- Post-Departure from Nucleate Boiling (DNB) brittle fracture of the clad material, which may take place during the re-wetting phase of the overheated heavily oxidised (and thereby embrittled) clad due to the abrupt quenching resulting in large thermal clad stresses.
- Cladding contact with molten fuel.

The failure mechanism for high burnup rods not subjected to DNB, is PCMI. The change in failure mechanisms for low burnup fuel is due to the decrease in pellet-cladding gap and the embrittlement of the cladding (due to corrosion induced hydriding) with increased burnup. The rapid increase in power leads to nearly adiabatic heating of the fuel pellets, which expand thermally and may cause fast straining and failure of the surrounding cladding through PCMI.

For high burnup rods with a rod internal gas pressure exceeding the coolant pressure that do not fail through PCMI may fail due to creep burst. A prerequisite for this failure mode is that heat transferred from the pellets at a later stage of the transient, may bring the clad outer surface to such a High Temperature (HT) that dry-out or DNB will occur. The elevated clad temperature may then lead to clad outward ballooning and creep burst failure.

Fuel dispersal – Provided that the cladding fails, fragmented fuel may disperse into the coolant [Lespiaux et al, 1997]. This expulsion of hot fuel material into water has a potential to cause rapid steam generation and pressure pulses, which could damage nearby fuel assemblies and possibly also the reactor pressure vessel and internal components. Hence, the potential consequences of fuel dispersal are of primary concern with respect to core and plant safety and therefore are not accepted by Regulators. Section 1.5 provides some best-estimate fuel rod energy and failure distribution calculations while the licensing criteria are described more in Section 1.6.

The failure limits established by the regulatory agencies are based mostly on the simulated RIA tests in the test reactors noted before. None of these reactors have the capability of reproducing an RIA precisely, however both CABRI and Nuclear Safety Research Reactor (NSRR) are modifying their test conditions to more closely simulate realistic RIA conditions. Their capabilities and results are discussed in Section 1.2. In a fresh fuel rod, the fissile material consists predominantly of ^{235}U , which is usually uniformly distributed in the fuel pellets. Hence, both power and fission products are generated with a relatively small variation along the fuel pellet radius. However, with increasing burnup, there is a non-uniform buildup of fissile plutonium isotopes through neutron capture by ^{238}U and formation of ^{239}Pu and heavier fissile isotopes of plutonium. Since the neutron capture takes place mainly at the pellet surface, the distributions of fissile material, fission rate and fission products will develop marked peaks at the pellet surface as fuel burnup increases. The shapes of these distributions are dependent not only on irradiation time, but also on the fuel initial content of ^{235}U , pellet radius and the neutron energy spectrum of the reactor. Figure 1-2 shows an example of the radial fuel temperature distribution for an intermediate/high burnup fuel rod and it is clear that the highest temperatures are occurring at the fuel pellet periphery.

RIA integral tests – The most reliable simulation of the RIA has been in test reactors that apply a power pulse to samples of irradiated fuel rods. The test reactors in France (CABRI), Japan (NSRR), Russia (IGR, BGR) and formerly in the US (SPERT, PBF) have produced a significant data base that has helped to establish the limits for a RIA. The test reactors can not provide conditions that exactly simulate the reactivity insertion due to a control ejection or control rod drop; however, modifications to the reactors as well as the modelling methods have made significant progress in this area as discussed in Section 1.2.

RIA modelling – Sophisticated modeling codes have been developed for evaluating these events, such as FALCON⁹ (EPRI¹⁰/ANATECH), SCANAIR (French), and FRAPTRAN (NRC¹¹/PNL). Evaluation and definition of the Design Base Accident (DBA) is on-going. The DBA is partly based on the ejection of the highest worth control rod and this can vary from one reactor to another and from one reload to another and can have significant effects on the predicted fuel performance. The accident initiation for PWRs is considered to occur at HZP and for BWRs at both HZP and CZP.

⁹ Fuel Analysis and Licensing Code

¹⁰ Electric Power Research Institute

¹¹ Nuclear Regulatory Commission

2 LOCA (Peter Rudling)

2.1 Introduction (Alfred Strasser and Peter Rudling)

The LOCA event starts by the decrease and then the loss of coolant flow due to a break in the coolant pipe, at the same time the reactor is depressurized, scrammed and shut-down. The fuel starts heating up due to its decay heat until the Emergency Core Cooling Systems (ECCSs) are activated and cools the fuel. Hypothetical LOCA events are analyzed for each reactor to assure that the safety criteria, defined by the regulators, for the reactor system and the fuel, are met. The DBA analyzed fall into two general categories. The large break, or Large Break Loss Of Coolant Accident (LBLOCA), assumes a double ended break of a primary coolant cold leg of a PWR or a break in the recirculation pump intake line of a BWR either of which could cause the loss of all the coolant from the core. The small break, or Small Break LOCA (SBLOCA), assumes a break in one of the smaller primary circuit lines that will cause less coolant loss than the LBLOCA.

The details and variables of the hypothetical accident and its effect on the fuel are described in Section 2.2.

A description of in-reactor and ex-reactor tests simulating LOCA are supplied in Section 2.3.

The effect of a LOCA cycle on the fuel is shown schematically on Figure 2-1, plotting the fuel and cladding temperatures as a function of time in the accident. The loss of coolant flow and reactor pressure at the initiation of the accident will decrease heat transfer and allow the fuel and cladding to heat up until the reactor scrams. The fuel will then cool down somewhat partly due to cooling by the steam-water mixture that is formed, but the cladding temperature will continue to rise.

During and after the LOCA it must be ensured that:

- The core remains coolable (which means that the maximum allowable coolant blockage is limited) and,
- no fuel dispersal occurs (which means that cladding rupture is not allowed; it is assumed that the cladding burst is so small that only fission gases are released).

The LOCA licensing criteria is discussed in Section 2.4.

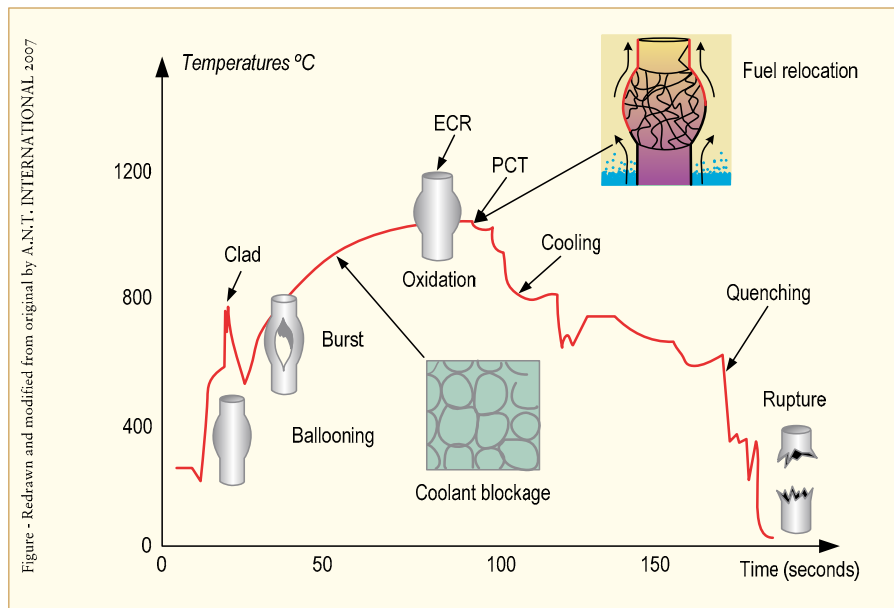


Figure 2-1: Typical LOCA in a PWR³¹.

In the following, the different phases the fuel rod goes through during a LOCA are described.

Ballooning – The loss of coolant flow decreases heat transfer from the fuel, increases the fuel temperature and causes a significant temperature rise of the cladding. The decrease in system pressure causes a pressure drop across and a hoop stress in the cladding. The result is the creep deformation, or *ballooning* of the cladding. Depending on the temperature, the cladding ductility and the rod internal pressure, the cladding will either stay intact or may *burst*. Ballooning of the fuel rods may result in *blockage* of the coolant sub-channel that in turn may impact the fuel coolability. If large fuel clad burst strains occur at the same axial elevation, *co-planar deformation*, in the fuel assembly, the coolability may be significantly degraded. Specifically, the clad azimuthal temperature gradient will strongly impact the burst strain, see Section 2.2.3.2.2 The fuel clad axial temperature distribution will determine the burst axial elevation of the fuel rods in the assembly. This axial and azimuthal fuel clad temperature distribution is in turn dependent on heat transfer mechanisms at the surfaces of the cladding. The extent of the ballooning is also dependent on:

- Creep strength of the cladding, dependant on:
 - Alloy composition
 - Microstructure
 - Texture
 - Oxidation during the LOCA
- Stress and corresponding strain rate the cladding is subjected to,
- temperature and the rate of temperature rise assumed for the DBA.

The most important safety criterion at this stage of the LOCA is that ballooned cladding should not cause coolant flow blockage that could impact fuel coolability. The distribution of the ballooned rod sections will depend on the axial and radial temperature distribution in the core. The worst case would be ballooning of the fuel rods in the same axial plane. However, ex-reactor multi-rod tests simulating ballooning events have not been able to produce a configuration that would restrict fuel cooling.

³¹ Fuel Material Technology report II, Chapter 4.

The potential relocation of cracked pellets in a ballooned region of the cladding during the heat-up phase of the LOCA cycle is an NRC concern since it could result in further clad expansion and coolant blockage. Experiments to resolve this issue are in progress.

Oxidation – The increasing temperatures and presence of steam will cause the intact cladding to oxidize on the OD and the burst cladding to oxidize on both the OD and ID (two sided oxidation). The oxidation process at the high LOCA temperatures will increase the oxygen and hydrogen content in the cladding, reducing its ductility and resistance to rupture. Two sided oxidation can have significant effects on the Post-Quench Ductility (PQD) of the cladding as a result of high, but localized hydrogen pick-up in addition to the oxidation.

The cladding continues to oxidize until the ECCS becomes effective and a PCT is reached. The maximum PCT is regulated to be a maximum of 2200 °F by the USNRC and 1200 °C internationally.

The length of time at the PCT is determined by the reactor system and regulated by the Equivalent Clad Reacted (ECR) limit, defined as the total thickness of cladding that would be converted to stoichiometric ZrO_2 from all the oxygen contained in the fuel cladding as ZrO_2 and oxygen in solid solution in the remaining metal phase. The USNRC's ECR limit at this time is 17% calculated in the past by the Baker-Just equation changed in the US to the Pawel-Cathcart equation by the NRC. Current regulations direct that the burst and ballooned cladding should be calculated for double sided oxidation and that pre-LOCA oxidation should be subtracted from the 17% total limit.

A third regulatory limit related to the oxidation phase is that the maximum amount of hydrogen generated by the oxidation reaction of the cladding will be 0.01 times (or 1% of) the hypothetical amount generated if all the cladding adjacent to the fuel columns were to react.

The oxide formed during the oxidation period is adherent and protective. However, after an extended period of time, generally beyond the typical LOCA cycle time, breakaway oxidation may occur when the protective oxide film cracks and exposes fresh cladding surface to the oxidizing atmosphere. The change in oxide film characteristics are accompanied by a change from parabolic to quasi-linear oxidation kinetics, a process that will further embrittle the cladding and reduce the PQD. The potential of *breakaway oxidation* during a LOCA has never been in question for western alloys, since that occurs at >3000 seconds at PCT compared to the LOCA cycle time of about 200 seconds, until the Russian E110 alloy, in a similar test, reached breakaway corrosion in <1000 seconds. Subsequent research indicated that the degradation in E110 corrosion resistance was due to fabrication related factors and that if the E110 was made from Kroll process zirconium sponge instead of the Russian electrolytic/iodide process and if the surface finish was improved by belt sanding instead of the Russian pickling process, the time to breakaway oxidation could be extended to that of western alloys. Nevertheless, the proposed current NRC regulations will require periodic qualification testing that all the alloys meet a minimum time to breakaway corrosion.

It is important to note that variables in the oxidation cycle as well as the subsequent cooling and quenching cycles assumed in the DBA will have a significant effect on the post-LOCA properties and these include:

- The rate of temperature increase to the PCT will affect the total oxidation.
- The oxidation of the cladding at the high LOCA temperatures will increase the oxygen content in the cladding, reducing its ductility and resistance to rupture.
- PCTs at <1200 °C will result in improved PQD.
- Decreased time at PCT will decrease the ECR and also improve PQD.

Cooling, quenching and embrittlement – The ECCS activation will stop the temperature rise and start cooling the core by injection from the bottom of the core in a PWR and from the top in a BWR. The “cooling” process as shown on Figure 2-1 is relatively slow until the emergency coolant contacts the fuel that has been at the PCT. At that point, in the range of 400° to 800 °C, identified as “quenching” in Figure 2-1 the water from the ECCS will reduce the cladding temperature at a rapid rate (1°–5 °C/sec) by re-wetting the cladding heat transfer surface. The process will collapse the vapor film on the cladding OD and cooling will be by nucleate boiling. Thermal shock due to the sudden change in heat transfer conditions can fracture the cladding at this stage and the ability of the cladding to withstand the thermal stresses will depend on the extent of oxidation and degree of cladding embrittlement that occurred during the LOCA transient.

The oxidation embrittlement process and final structure of the cladding after completion of the LOCA cycle is shown on Figure 2-2 and the process is as follows:

- First, the increasing water and steam temperatures during heat-up increase the reaction rates with the cladding and increase the conversion of the cladding surface into thicker ZrO_2 films.
- As the LOCA temperature passes the levels where $\alpha \rightarrow \beta$ transformations start and finish, shown in Figure 2-3 for Zircaloy 4 and M5, the resulting structure consists of:
 - The growing ZrO_2 layer,
 - a zirconium alloy layer with a very high oxygen content which stabilizes the α phase,
 - the bulk cladding which is now in the β phase.
- The ECCS initiated quenching phase cools the cladding back down through the $\beta \rightarrow \alpha$ transformation temperature and the bulk cladding is now re-transformed from the β into the α phase and referred to as the “prior or former β phase”.

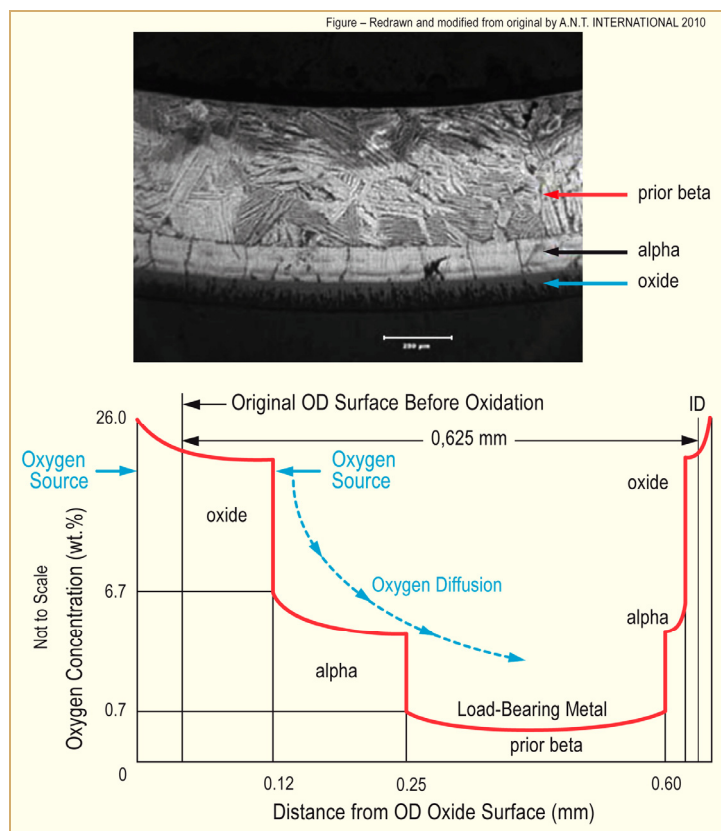


Figure 2-2: Structure of oxidized cladding [Meyer, 2005], (The presence of Nb would result in a similar structure except the boundary between the alpha and the prior beta phase would be more uneven).

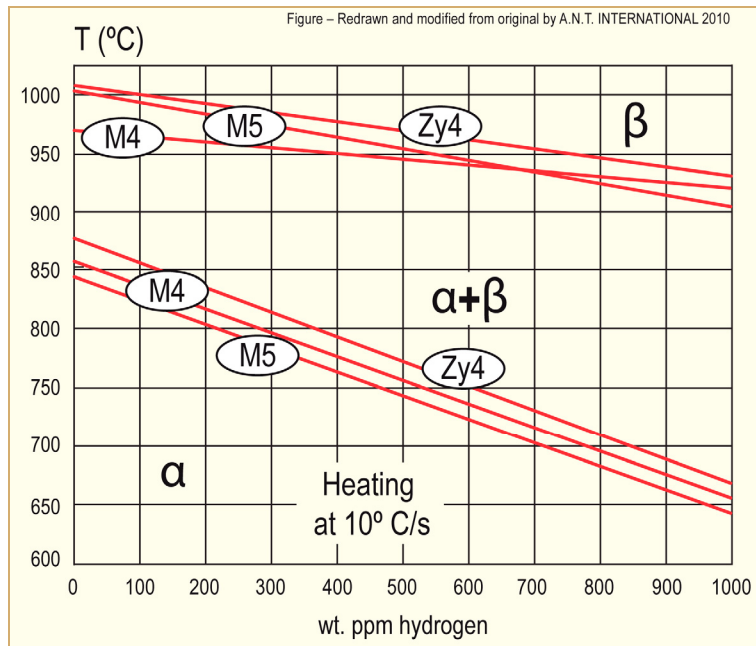


Figure 2-3: The phase transformation temperatures of Zry-4, M4 and M5 alloys as a function of the hydrogen content for a heating rate of 10 °C/s [Brachet et al, 2002].

Oxygen and hydrogen affect the formation of the structure as follows during the oxidation:

- Oxygen diffuses from the ZrO_2 to the bulk cladding which is in the β phase at the HT; however, the β phase has a low solubility for oxygen.
- Increased hydrogen levels from the oxidation reactions prior to and during the LOCA increase the diffusion rate and solubility of oxygen in the β phase >1000 °C.
- Wherever the solubility limit of oxygen in the β phase is exceeded, the excess oxygen stabilizes the α phase.
- The oxygen stabilized alpha phase forms next to the ZrO_2 layer and grows, as does the ZrO_2 layer, at the expense of the bulk cladding in the β phase and as a result after quenching in the “prior β phase”.

The final integrity of the cladding is based on the properties of the prior β phase, since the ZrO_2 and oxygen stabilized α zones are too brittle to sustain a load. The embrittlement criteria are based on properties measured on post-simulated LOCA tests of the various alloys by various test methods discussed in Section 1.2.2.

Again, it is important to note that variables assumed for cooling and quenching during the DBA will have a significant effect on the degree of embrittlement and the PQD:

- Slow cooling rates from the PCT to the quenching temperature will increase the PQD.
- Lower quenching temperatures, such as 600 °C, instead of 800 °C will increase the PQD.
- Lower quenching rates from the quenching temperature will also increase the PQD.

Oxygen is the major source of cladding embrittlement as noted above and hydrogen is less likely to contribute to the embrittlement except to the extent that its presence increased the oxygen solubility. The post-quench properties of the various claddings are discussed in Section 2.2.6.

Since the mechanical properties of the prior β zone could change as a function of extended burnup and increased oxygen and hydrogen contents, the USNRC and other organizations are evaluating the effects of extended burnup on its properties and the potential need for changing the criteria. The objectives of the current modifications planned by the NRC are to make the criteria material independent, and independent of %ECR while maintaining the PCT. The main objective is to preserve a certain amount of PQD in order to prevent fuel ruptures and flow blockage and maintain coolability of the core after a LOCA event. The current criterion proposed by the NRC in its LOCA Workshop of April 28-29, 2010 is based on meeting pre-LOCA hydrogen content related to ECR and having their combination be within the DBT zone as shown in Figure 2-4. This figure is still the subject of negotiation. More information about LOCA licensing appears in Section 2.4.

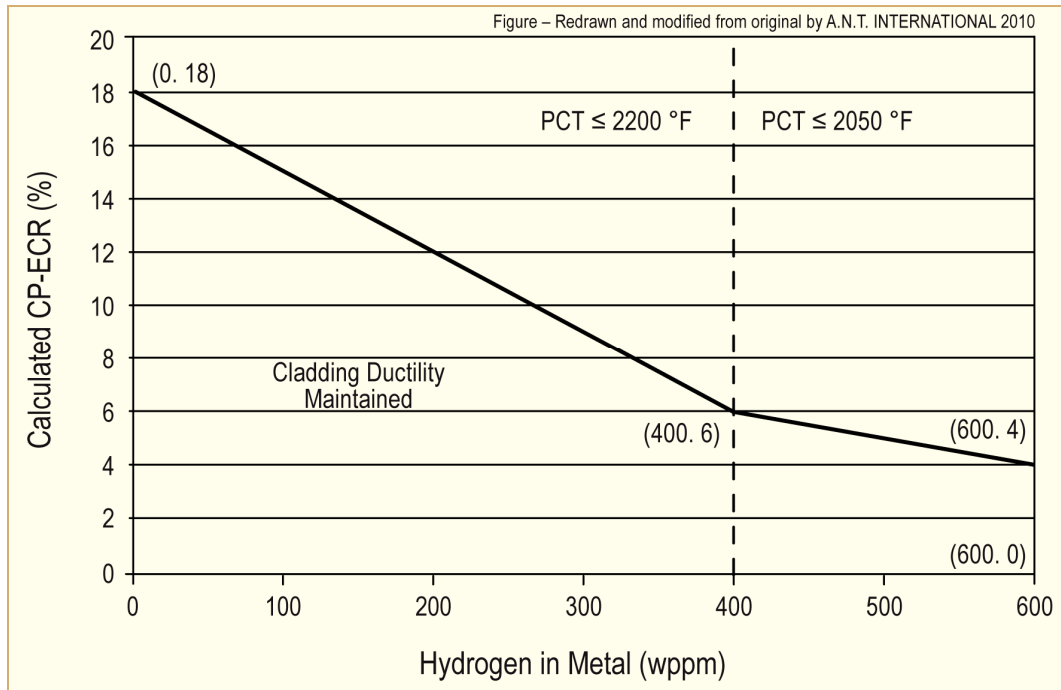


Figure 2-4: Ductile-to-brittle transition as a function of oxidation and hydrogen level.

The following topics are discussed more in the subsequent Sections:

- The impact of various parameters on LOCA fuel performance in Section 2.2,
- ex- and in-reactor tests simulating LOCA in Section 2.3 and,
- LOCA licensing criteria in Section 2.4.

2.2.6.3 Effect of PCT

Figure 2-56 and Figure 2-57 show that for a constant oxidation temperature, an increased degree of oxidation, i.e., increased ECR, also decreases failure impact energy/ductility of the cladding. These figures also show that increasing sample oxidation temperatures at constant ECR also increases the clad embrittlement. This is due to increased oxygen solid-solution hardening of the prior-beta phase with increased temperature (Figure 2-57). As mentioned earlier, the 1204 °C PCT limit was selected on the basis of slow-RCTs that were performed at 25-150 °C. The PQD and toughness of the cladding material are determined primarily by the thickness and the mechanical properties of the transformed-beta layer.

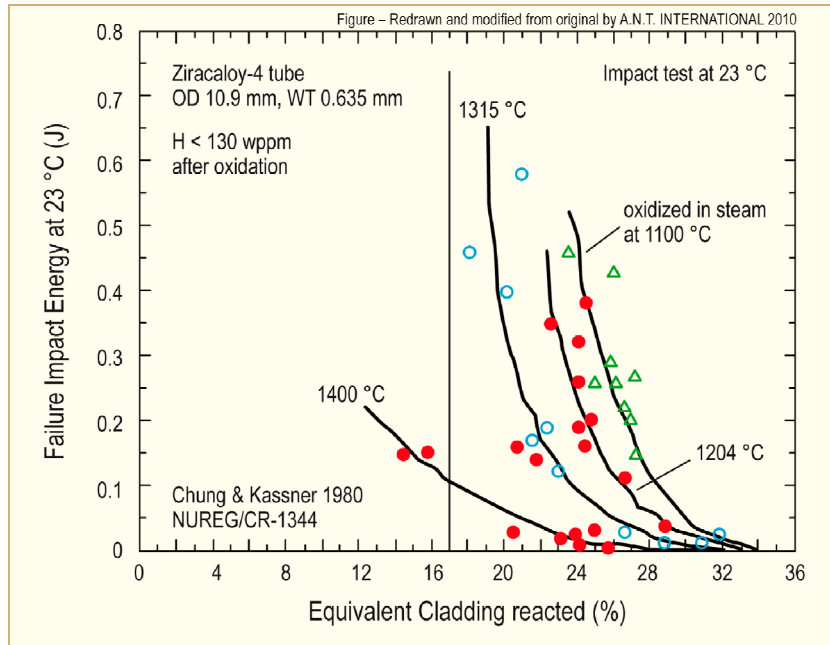


Figure 2-56: Failure impact energy vs. ECR, from tests at 23 °C on undeformed Zircaloy-4 tube oxidized on two-sides and cooled at 5 °C/s [Chung & Kassner, 1980].

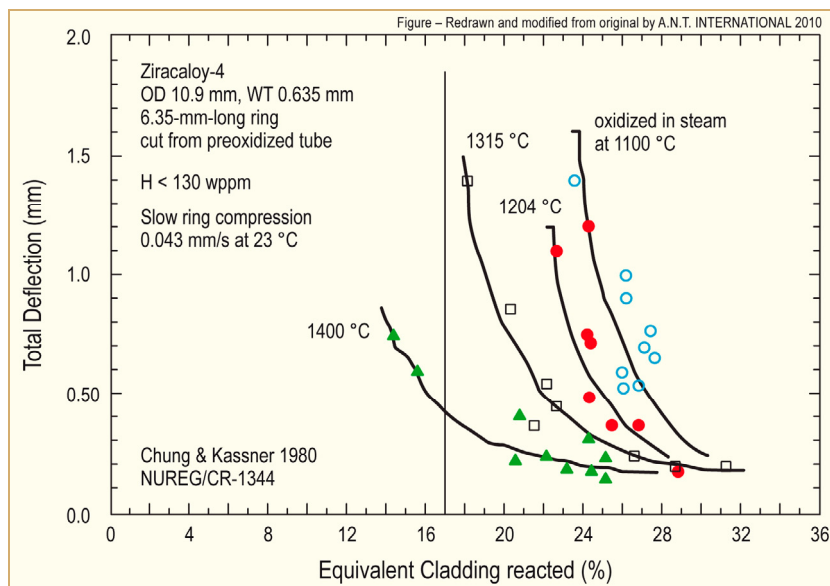


Figure 2-57: Total deflection in a RCT at 23 °C vs. ECR, from ring-compression tests on Zircaloy-4 oxidized on two-sides and cooled at 5 °C/s [Chung & Kassner, 1980].

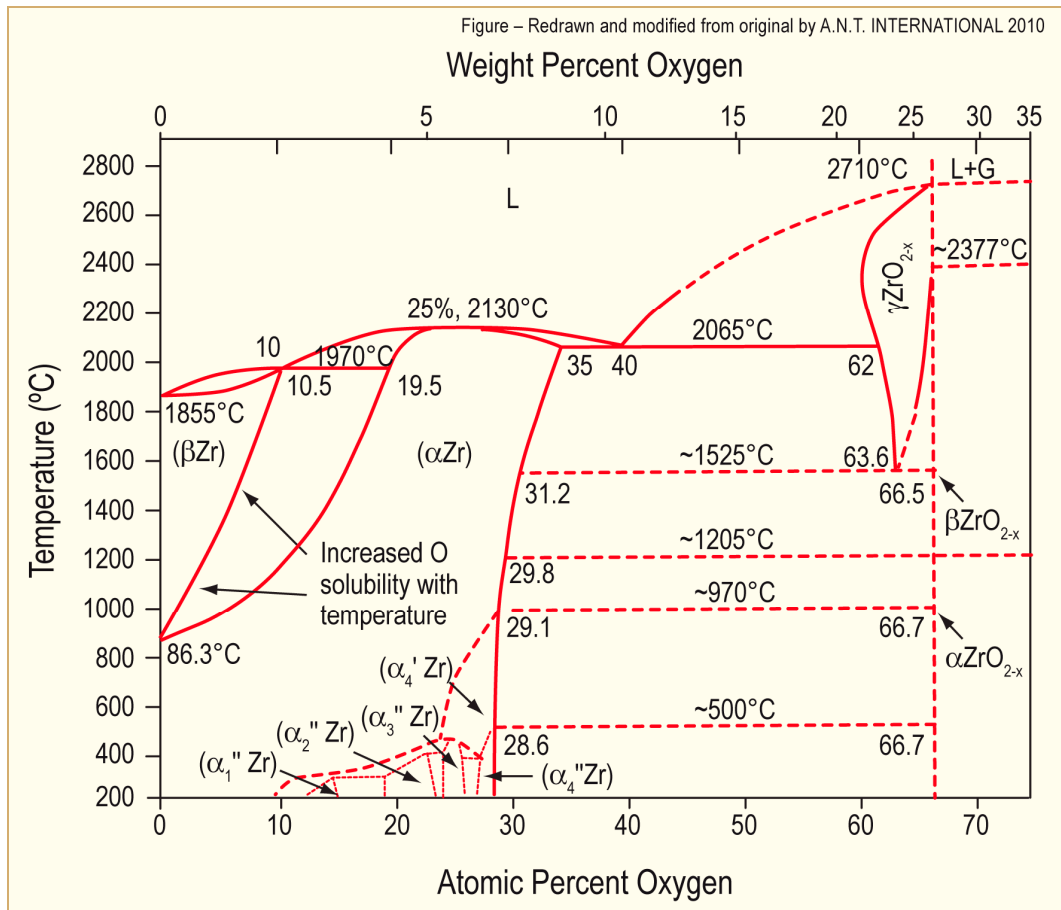


Figure 2-58: Zr-O phase diagram, modified figure according to [Abriata et al, 1986].

2.2.6.4 Effect of fuel-clad bonding

There is currently a debate if the ZrO₂ at the clad ID that exists in fuel with fuel-clad bonding can form an α -Zr stabilised layer at the clad inner surface through inward diffusion of oxygen from the ZrO₂ into the cladding wall during the LOCA oxidation or not. If the ZrO₂ oxide at the clad inner surface indeed can cause formation of an α -Zr stabilised layer at the clad inner surface, this effect will further embrittle the cladding and reduce the margin to rupture during quenching and/or post-LOCA event.

More work is needed to resolve this issue as it could have a direct effect on the allowable, pre-transient oxidation.

2.2.6.5 Effect of quenching

The effect of cooling rates were tested on the PQD of Zr-4 cladding samples that were prehydrided to 600 ppm hydrogen, preoxidized at 1200 °C for 50s and then quenched from 1200°, 800°, 700° and 600 °C. The results of RCT and 3-PBT⁴³ at 135 °C showed:

- Almost no plasticity after a slow cool to the 800 °C quench temperature or a direct quench from 1200 °C.
- Increased plasticity after slow cool to quench temperatures of 700° and 600 °C or slow cool from 1200 °C.
- Higher plasticity for the 700° and 600 °C quenched samples than the continuous slow cooled one from 1200 °C.

The variation in load and offset strain (ductility) as a function of the cooling sequence are shown on Figure 2-59. The explanation of the unusual, improved plasticity of the 700° and 600 °C quenched samples lies in the fact that the $\beta \rightarrow \alpha$ transformation is complete before the quench and the microstructure is modified by the partitioning of oxygen, hydrogen and the alloying elements. The partitioning of oxygen was described by Stern (Figure 2-60 and Figure 2-61). The slow cooling rate from the oxidation temperature to RT has given time for some coarse hydrides to precipitate and this is believed to be the cause of the low ductility for these samples.

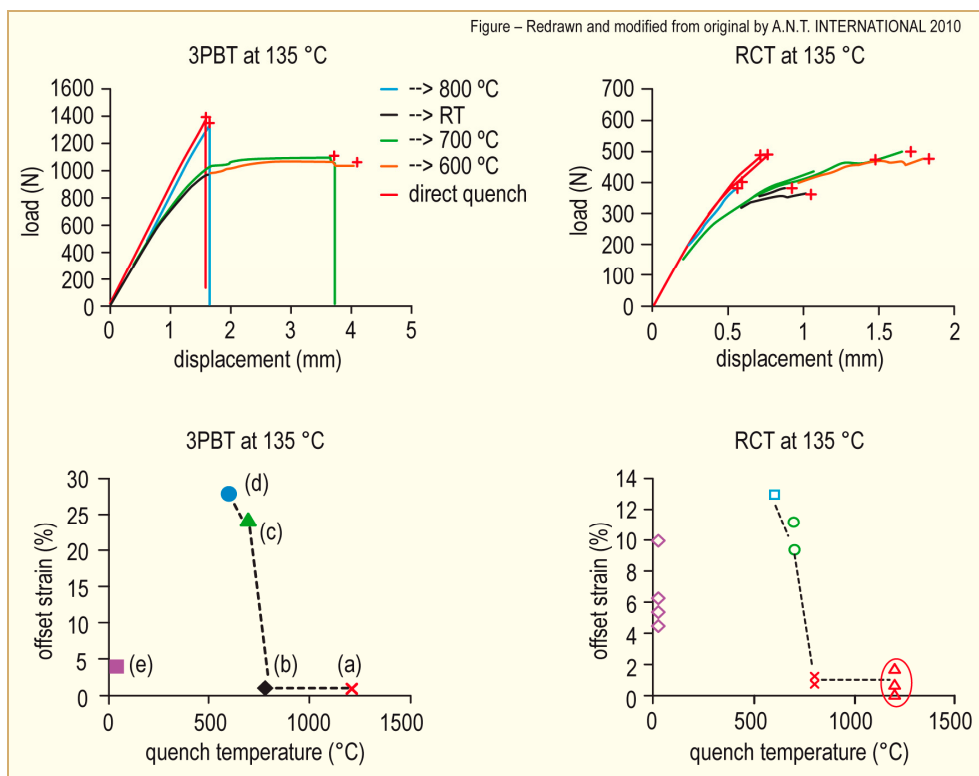


Figure 2-59: Effect of cooling sequence on Zr-4 with 600 ppm hydrogen oxidized at 1200 °C [Brachet et al, 2007].

⁴³ Point Bend Test

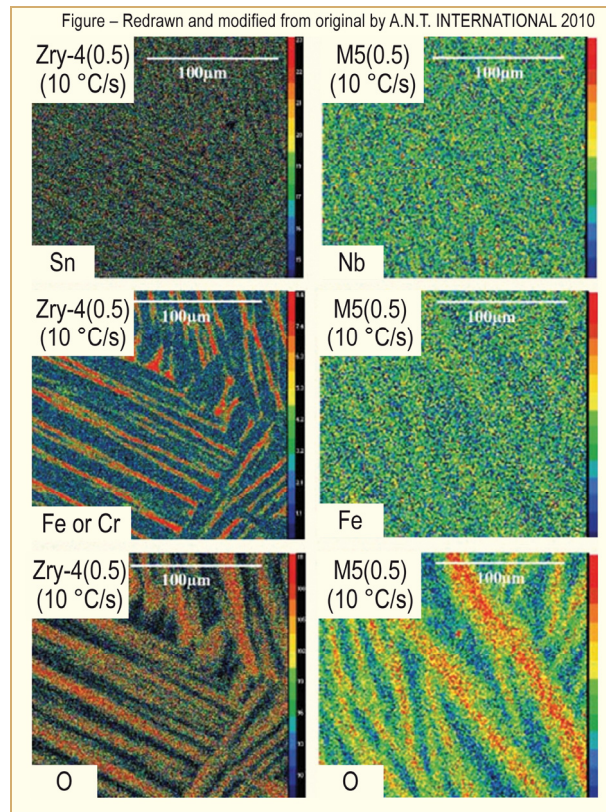


Figure 2-60: EPMA mapping of elements after cooling at 10 °C/s of Zr-4 and M5 [Stern et al, 2007].

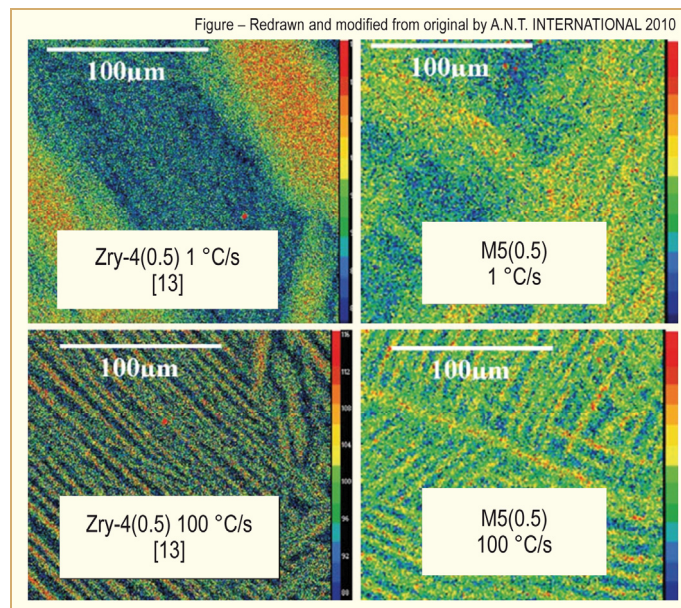


Figure 2-61: EPMA oxygen mapping for 0.5% oxygen Zr-4 and M5 at slow and fast cooling rates [Stern et al, 2007].

Fractographic evidence supports the mechanical test data (Figure 2-62). The cleavage facets on the specimens quenched from 800 °C indicate brittle failure and the lower temperature quenched specimens' flat dimples indicate a more ductile failure. Secondary cracks observed in the specimens slow cooled from the oxidation temperature to RT were believed to be due to the hydride formation and embrittlement.

Microhardness measurements made on specimens quenched from 800° and 700 °C confirmed the mechanical property trends (Figure 2-63). The hardness of the prior β zone after the 800 °C quench is considerably harder than the one from the 700 °C quench, indicating a lower ductility.

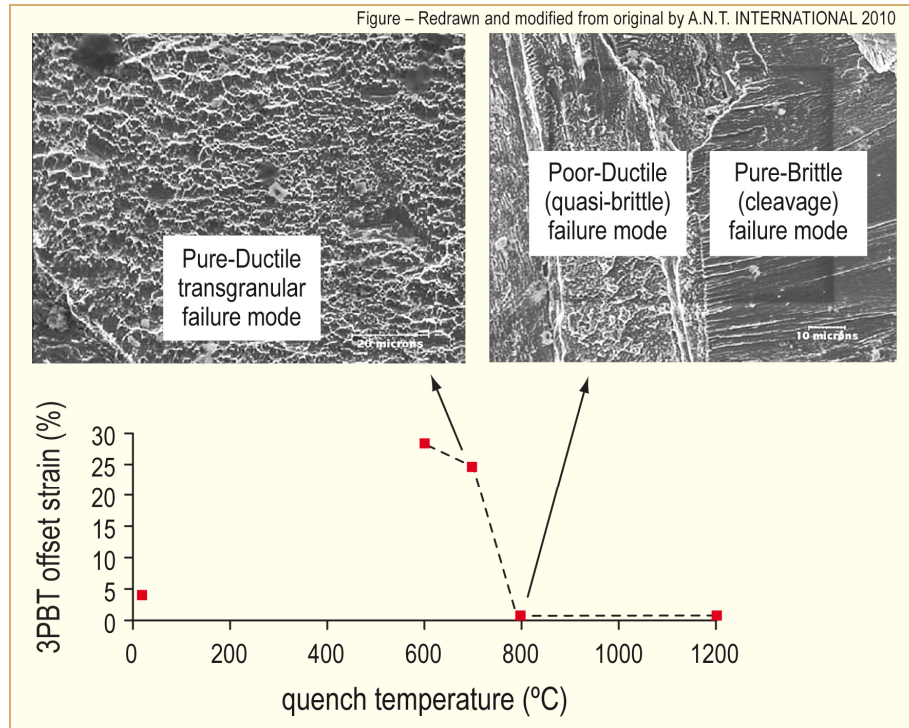


Figure 2-62: Fractographs of Zr-4 3-PBT specimens [Brachet et al, 2007].

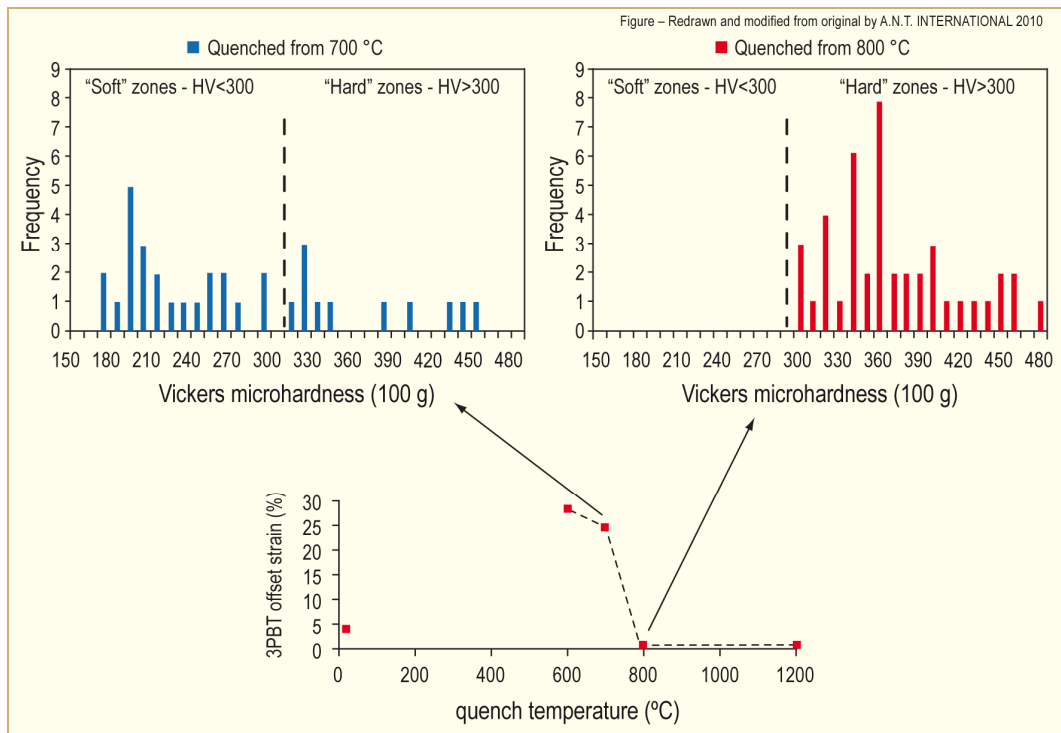


Figure 2-63: Microhardness of the Zr-4 prior β zone as a function of quench temperature [Brachet et al, 2007].

2.2.6.6 Effect of stress (fuel rod restraint)

The influence of axial restraint on the fracture behaviour of unirradiated Zry-4 cladding samples was evaluated relative to hydrogen concentration [Nagase & Fuketa 2004]. This study defined the threshold for fracture due to axial restraint during quenching in terms of ECR as calculated by the Baker-Just equation. The results, shown in Figure 2-66 and Figure 2-67, indicate that the ECR fracture threshold decreases with the amount of axial restraint and, when restraint is present, with the amount of hydrogen.

Additional information on the fracture behaviour of irradiated Zircaloy-4 fuel claddings was presented by Fuketa in the IAEA meeting in Kendal, England. These results are summarised in Table 2-3 and depicted in Figure 2-66 [Fuketa et al, 2005]. As can be seen, the effect of hydrogen on irradiated and unirradiated claddings are similar. This indicates that hydrogen is one main contributors to failure and that irradiation-induced damage as such is a lower-order contributor, at least up to a burnup level of 44 MWd/kgU. Figure 2-67 shows the post-test appearance of irradiated fuel cladding which fractured during quenching. Fuketa and company consider that the crack initiated at the rupture opening and propagated circumferentially. Fuketa notes that hydrogen concentration close to the rupture opening is around 1500 wppm, which is much higher than the initial value. He believes that the clad is ruptured by both oxidation and hydriding phenomenon.

Fuketa remarked that that JAERI will continue to perform LOCA-related investigations on PWR and BWR claddings (Zircaloy-2, MDA, NDA, ZIRLO and M5) irradiated to about 70 MWd/kgU.

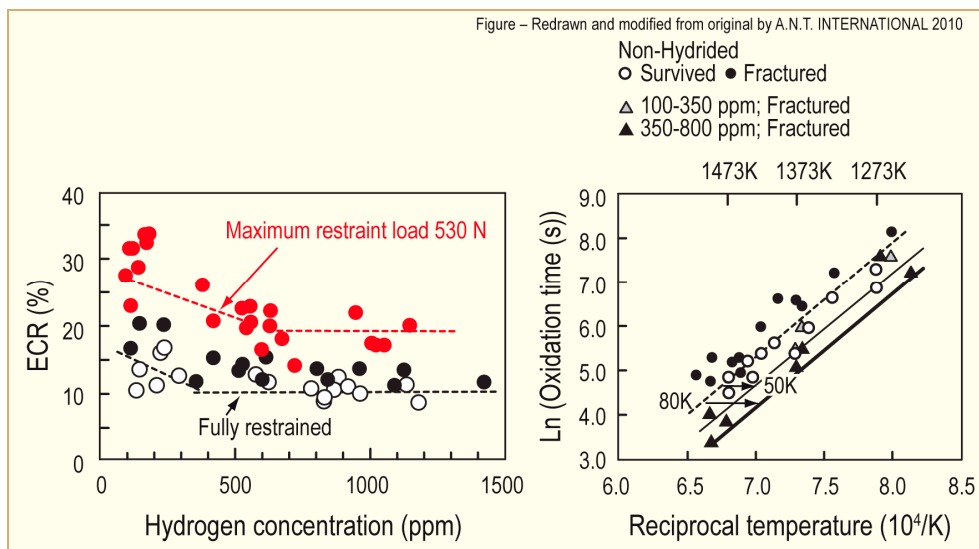


Figure 2-64: Hydrogen effect on fracture under simulated LOCA condition (unirradiated Zircaloy-4 clad). The diagram on the left shows the effect of restraint on the ECR for fracture relative to hydrogen concentration. The diagram on the right shows the effect of hydrogen on fracture relative to oxidation time and temperature under full restraint [Nagase & Fuketa, 2004].

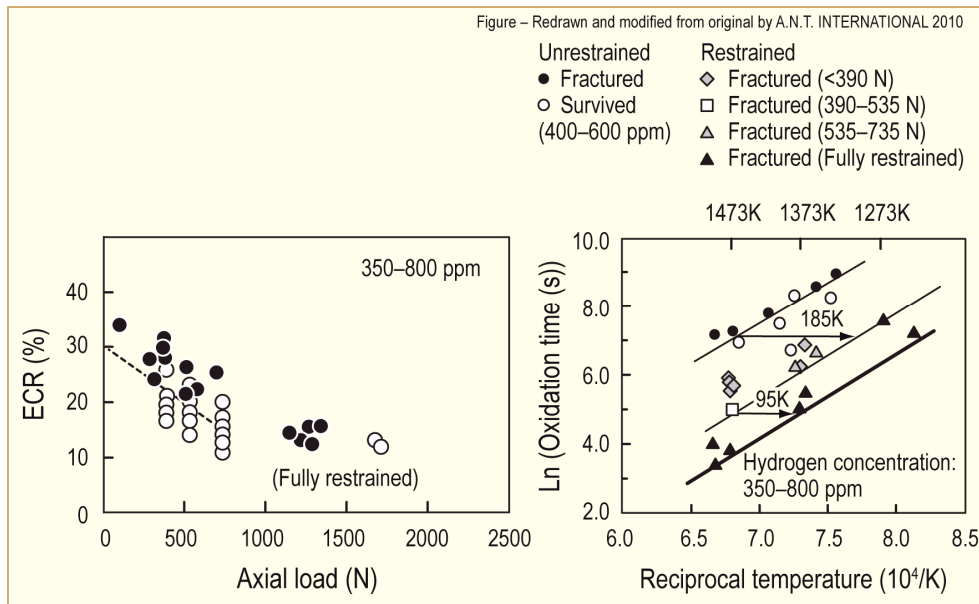


Figure 2-65: Influence of restraint load on fracture under simulated LOCA condition (unirradiated hydrided Zircaloy-4 clad). The diagram on the left shows the effect of restraint load on the ECR for fracture. The diagram on the right depicts fracture behaviour relative to oxidation time and temperature for several restraining loads [Nagase & Fuketa, 2004].

Table 2-3: Summary of integral tests performed on Zircaloy-4 PWR clad. Here B_u is the rod burnup, w_{ox} initial oxide thickness, C_H estimated initial hydrogen content, T_{ox} oxide temperature, t_{ox} oxidation time, L_f load at fracture [Fuketa et al, 2005].

Test No	Unit	1	2	3	4	5	6
B_u	MWd/kgU	43.9	39.1	40.9	43.9	39.1	40.9
w_{ox}	μm	20	15	18	25	18	15
C_H	wppm	170	120	140	210	140	120
T_{ox}	K	1449	1450	1445	1451	1427	1303
t_{ox}	s	486	543	363	120	200	2195
ECR*	%	29	26	21	17	16	22
Status	---	Failed	Failed	Intact	Intact	Intact	Intact
L_f	N	498	385	---			

* Based on clad thickness after ballooning and rupture.

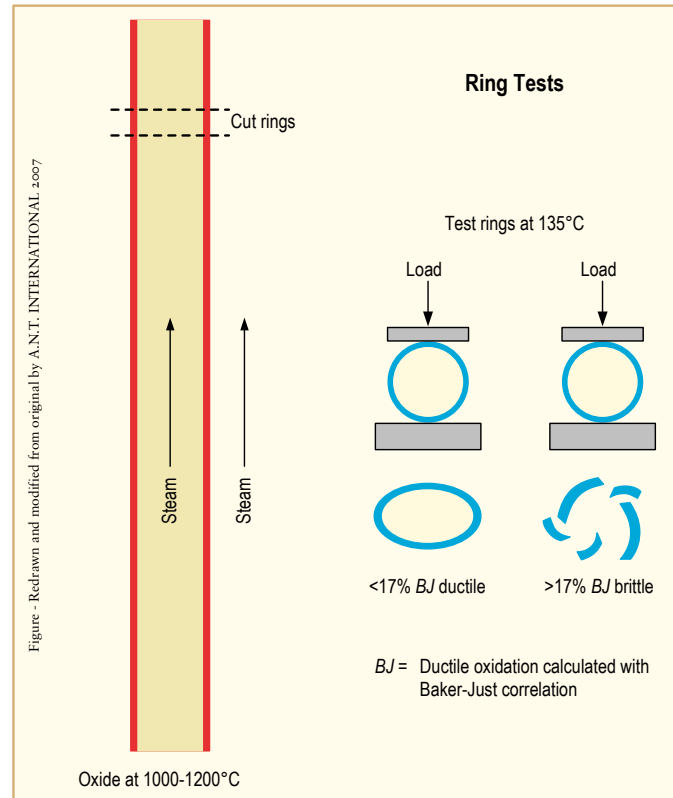


Figure 2-68: Diagram of Hobson-type ring-compression tests used to obtain current LOCA embrittlement criteria [Meyer, 2003].

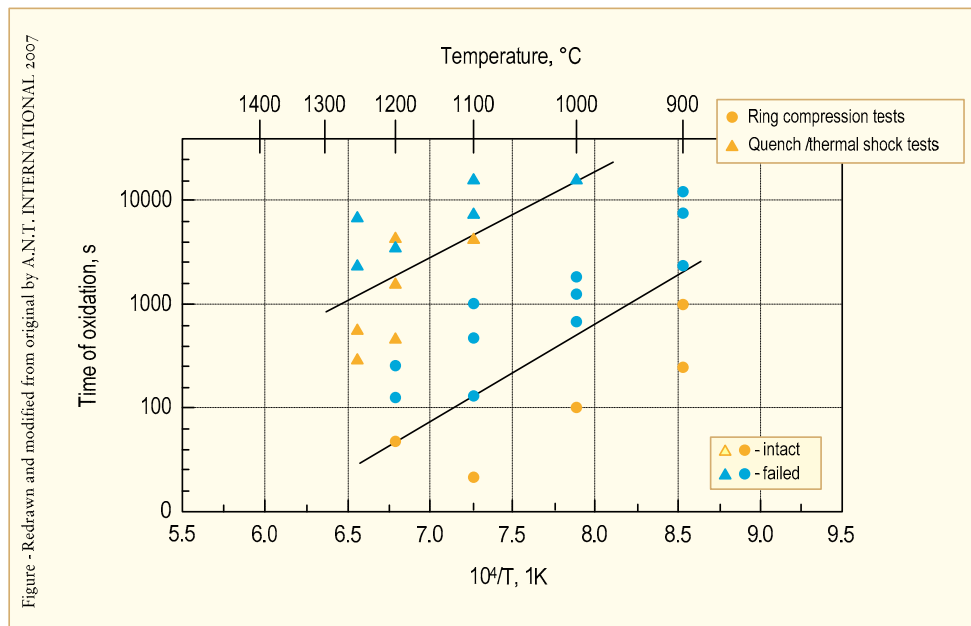


Figure 2-69: Cladding "failure" test data obtained in quench test and in RCTs on the same cladding material and in the same laboratory. As shown, the compression/brittleness tests give a far lower safety limit, typically ~250 °C lower [Maroti, 2001].

The major reason that the cold compression test is more conservative has to do with the impact of hydrides on ductility at different temperatures. At higher temperatures, the embrittlement effect of hydrides is much less than at lower temperatures.

2.4 Licensing LOCA criteria

The overall objective of reactor safety is the prevention of radiation-related damage to the public from the operation of commercial nuclear reactors.

The LOCA and RIA work done during the 60s and 70s were formalised in the legislating documents produced by the Nuclear Regulatory Commission in USA, USNRC. There are two parts of the legislating documents that have relevance to LOCA and RIA, namely, [10CFR Part 50 Appendix A] and [10CFR100, NRC]. The Standard Review Plan, NUREG-0800, USNRC, is used by NRC regulators to interpret 10CFR50, and 10CFR100. The main objective of 10CFR50 and 10CFR100 is to limit radioactive impact on the environment, as follows:

- In 10CFR100, it is specified that conservative dose calculations must be done to assess the potential impact on the environment during a DBA.
- In 10CFR50, the General Design Criteria, GDCs are specified and interpreted in SRP Section 4.2-4.4, which imposes mechanical, nuclear and thermal hydraulic fuel design criteria that the fuel vendor and the utility must meet.

These regulations are described more in the following subsections.

2.4.1 10CFR100

Fission products must be adequately considered as the radioactive *source term*⁴⁷ in case of a nuclear incident and/or accident. From a regulatory point of view some of this radioactivity will leak out of the containment and reach the environment outside the nuclear plant where it will cause a dose burden to the public.

With knowledge of fission product distributions in the containment atmosphere and reliable estimates of the number of failed fuel rods it would in principle be possible to reach reasonably realistic numbers for the in-containment source term.

The fraction of burst failed fuel was reported in joint European study [EUR 19256EN, 1999]. On the basis of the mechanistic analyses participants in the project determined burst failure thresholds for the fuel. The best estimate failure threshold is shown in Figure 2-78. Based on the failure thresholds, the failed fuel fraction was calculated. Table 2-5 shows that the best estimate analysis resulted in zero fraction of failed fuel in all but one case.

In more conservative estimate, the failure threshold lies about 50-150 W/cm lower than the curves shown in Figure 2-78, resulting in calculated failed fuel fractions between 0 and 16.6% [EUR 19256EN, 1999]. For reactors with injection into both hot and cold legs⁴⁸, a failed fuel fraction of 10% was calculated with this conservative approach. In the German licensing methodology a maximum of 10% burst failed fuel rods is accepted in the core.

⁴⁷ During and immediately following an accident, the part of the fission product inventory, released into the containment, potentially available for the release to the environment is called the source term

⁴⁸ Hot and cold leg injection leads to lower fuel temperature and fewer failed rods during a LBLOCA.

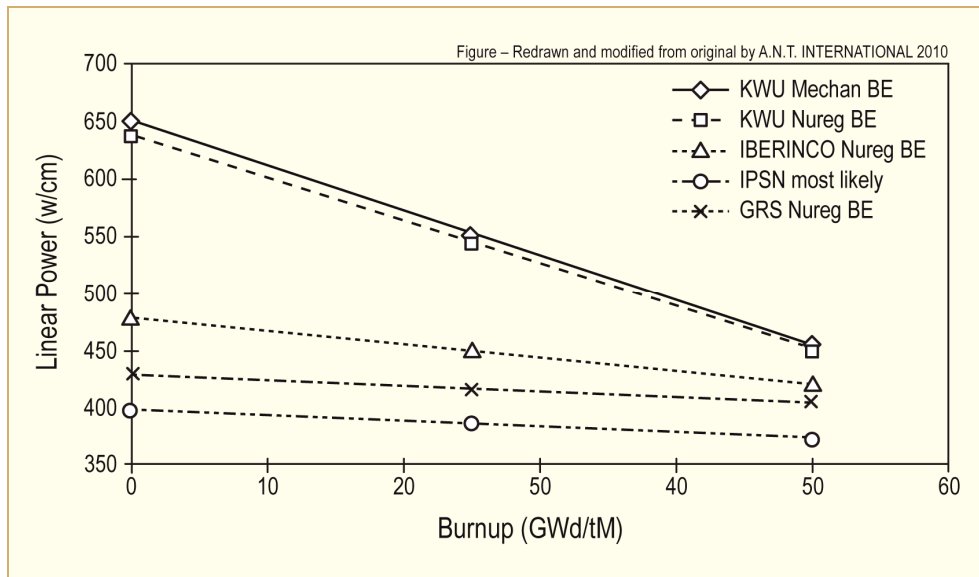


Figure 2-78: Best estimate burst failure thresholds for PWR fuel in a large break LOCA (upper two curves) and corresponding conservative thresholds (lower three curves) [EUR 19256EN, 1999].

Table 2-5: Best estimate analyses of percentage of fuel rod failures [Bratby et al, 1999].

Participants	Boundary conditions	Rupture criterion	Failed fuel fraction (%)
NNC	Best Estimate	NUREG-0630 B.E.	0
EdF	Cons./B.E.	NUREG-0630 B.E.	0
EdF	Cons./B.E.	EDGAR bundle	0
IBERINCO	Conservative	NUREG-0630 B.E.	0
GRS (UO ₂)	Conservative	NUREG-0630 B.E.	3.2
Siemens	Best Estimate	Mechanistic B.E.	0
Siemens	Best Estimate	NUREG-0630 B.E.	0
NRG	Best Estimate	NUREG-0630 B.E.	0

The application of these findings varies among regulatory agencies. In the United States, for instance, 100% of the fuel rods are assumed to fail as a result of a LOCA and the containment is required to retain most of the fission products. The dose calculations for all the other DBAs are calculated based upon the results of the DBA analysis. For RIA, a conservative assumption is used that all rods, which experienced a surface heat flux in excess of the DNBR (in PWRs) and CPR (in BWRs) have failed. For the dose calculations, only the source term generated by these assumed failed rods need to be taken into account. Historically, NRC has defined that during a RIA, the dose must be within 25% of the 10CFR100 dose limits. For other DBAs (other than LBLOCA and RIA), NRC has licensed plants to specific requirements, normally 10% of the 10CFR100 limits. The reasons for the difference in maximum allowable dose for different DBAs is that in the case of e.g. a LOCA, there is some delay in the radioactivity leaking out to the environment while for other accidents (with lower maximum allowable doses) such as steam generator tube rupture, there is a direct path of the radioactivity to the environment.

In Sweden dose calculations are not done for LBLOCA since all Swedish NPPs are equipped with a filter that essentially eliminates any spread of activity to the environment during these types of accidents. Also in France these type of dose calculations are not performed. As mentioned earlier in Germany it must shown that less than 10% of the fuel has failed during a LOCA and the number 10%⁴⁹ is then used in the dose calculations. In Germany it must shown, by code calculations that less than 10% of the fuel has failed during a LOCA. However, even though the calculated number of failed rods is less than 10%, the 10% number must be used in the dose calculations to be conservative.

2.4.2 10CFR50 (ECCS criteria)

The main objective of the ECCS criteria established by the regulators is to maintain core coolability.

Current US regulations

The current regulations intend that modelling of the hypothetical accident will show that rupture of the cladding during the quenching process can be prevented by the application of the regulatory limits. The USNRC's regulatory limits for LOCA are stated in 10CFR Part50, paragraph 50.46 and are summarized briefly as:

- The maximum fuel cladding temperature shall not exceed 2200 °F (1204 °C).
- Oxidation of the cladding should not exceed 17% (ECR< 17%) of the cladding thickness at any point of the fuel rod:
 - a) The pre-LOCA oxidation should be subtracted from the 17% total oxidation.
 - b) For ruptured and ballooned cladding the calculation should be for double sided oxidation.
- Calculations must indicate that a coolable geometry is maintained in the core⁵⁰.
- The maximum amount of hydrogen generated by the oxidation reaction of the cladding will be 0.01 times the hypothetical amount generated if all the cladding adjacent to the fuel column were to react.
- Applicable cladding alloys are Zircaloy 2, Zircaloy 4 and ZIRLO.

⁴⁹ Siemens built reactors have Emergency Core Cooling (ECC) water injection into both hot and cold legs which reduces the fuel temperatures thus reducing the number of failed rods and therefore a failed fuel fraction of 10% was supported which is the same at that adopted in the German, licensing methodology. Other reactor designs have only ECC water injection in the cold leg only, leading to higher fuel temperatures. In these reactors, 100% of the fuel are assumed to have failed during a LBLOCA.

⁵⁰ The coolable geometry may be lost by either fuel clad ballooning causing coolant channel blockage or fuel cladding fragmentation due to clad embrittlement. After any operation of the ECCS, the core temperature shall be maintained at an acceptably low value and decay heat removed for the extended period of time required by long-lived radioactivity.

3 References

- 10CFR Part 50 Appendix A, *General Design Criteria for Nuclear Power Plants*, USNRC, Washington, 1990.
- 10CFR Part 100.11, *Determination of Exclusion Area, Low Population Zone, and Population Centre Distance*, U.S. Government Printing Office, Washington, 1990.
- 10CFR100, NRC, Standard Review Plan, NUREG-0800, USNRC, 1995
- Abriata J. P. Garces J. and Versaci R., *Bull. Alloy Phase Diagrams* 7(2), pp. 116-124, 1986.
- Adamson M. G., Aitken E. A. and Caputi R. W., *Experimental and thermodynamic evaluation of the melting behavior of irradiated oxide fuels*, *Journal of Nuclear Materials*, Vol. 130, pp. 349-365, 1985.
- Adamson R. B. et al, *High Burnup Fuel Issues*, ZIRAT8/IZNA3 Special Topics Report, ANT International, Skultuna, Sweden, 2003/2004.
- Agee L. J., Dias A. F., Eisenhart L. D. and Engel R. E., *Realistic scoping study of reactivity insertion accidents for a typical PWR and BWR core*, Proc. CSNI specialist meeting on transient behaviour of high burnup fuel, pp 291-304, Cadarache, France, September 12-14, 1995.
- Andersson, T. and Wilson A., *Ductility of Zircaloy canning tubes in relation to stress ratio in biaxial testing* In: *Zirconium in the nuclear industry; 4th international symposium*, J. H. Schemel and T. P. Papazoglou, Editors, American Society for Testing and Materials, ASTM STP-681, pp. 60-71, 1979.
- ANS, *American National Standard for Decay Heat Power in Light Water Reactors*, ANSI/ANS-5.1, American Nuclear Society, 2005.
- Asmolv V. et al, *Understanding LOCA-Related Ductility In E110 Cladding*, Proc: 30th Nuclear Safety Conference, Washington, DC, USA, October, 2002.
- Bai J. B., *Influence of an oxide layer on the hydride embrittlement in Zircaloy-4*, *Scripta Metallurgica at Material*, 29, pp. 617-622, 1993.
- Baker L. and Just L. C., *Studies of metal-water reactions at high temperatures. III. Experimental and theoretical studies of the zirconium-water reaction*, ANL 6548, May 1962.
- Bender D. et al, *Methodology and results of RIA studies at Siemens*, In: CSNI specialist meeting on transient behaviour of high burnup fuel, OECD Nuclear Energy Agency, NEA/CSNI/R(95)22, pp. 305-314, Cadarache, France, September 12-14, 1995.
- Bessiron V., T. Sugiyama and Fuketa T., *Clad-to-coolant heat transfer in NSRR experiments*, *Journal of Nuclear Science and Technology*, 44(5): pp. 723-732, 2007.
- Bibilashvili Y. K. et al, *WWER-1000 type fuel assembly tests on electroheated facilities in LOCA simulating conditions*, IAEA Technical Committee Meeting on Fuel behaviour under transient and LOCA conditions, pp. 169-185, Halden, Norway, 2001.
- Boyack B. E. et al, *Phenomenon identification and ranking tables (PIRTs) for rod ejection accidents in pressurized water reactors containing high burnup fuel*, NUREG/CR-6742, US Nuclear Regulatory Commission, Washington DC, USA, 2001.
- Brachet J. C. et al, *Influence of hydrogen content on the α/β phase transformation temperatures and on the thermal-mechanical behaviour of Zry-4, M4 and M5 (ZrNbO) alloys during the first phase of LOCA transient*, *Zirconium in the Nuclear Industry: Thirteenth International Symposium*, ASTM STP 1423, G. D. Moan and P. Rudling, Eds., ASTM International, West Conshohocken, PA, 2002.

- Brachet J. et al, *Hydrogen Content, Pre-Oxidation and Cooling Scenario Influences on Post-Quench Mechanical Properties of Zy-4 and M5 Alloys in LOCA Conditions – Relationship with the Post-Quench Microstructure*, 15th Int. Conf. on Zirconium in the Nuclear Industry, ASTM, Sun River, Oregon, June, 2007.
- Bratby P. A. W., Dutton L. M. C. and Sutherland L., *Fuel cladding failures following a large LOCA*, NNC Report C5665/TR/006, Issue 01, May 1999.
- Carbajo J. J. and Siegel A. D., *Review and comparison among the different models for rewetting in LWRs*, Nuclear Engineering and Design, 58, pp. 33-44, 1980.
- Carbajo J., Yoder G., Popovb S., and Ivanov V., *A review of the thermophysical properties of MOX and UO₂ fuels* Journal of Nuclear Materials, Vol. 299, pp. 181-198, 2001.
- Carey V. P., *Liquid-vapor phase-change phenomena: An introduction to the thermophysics of vaporization and condensation processes in heat transfer equipment*, 2 ed., Taylor & Francis, Washington, USA, 2007.
- Cazalis B. et al, *The PROMETRA Program: Fuel Cladding Mechanical Behavior Under High Strain Rate*, Nuclear Technology, p. 215-229, vol. 157, March, 2007.
- Chapin D. L. et al, *Optimized ZIRLO Qualification Program for EdF Reactors*, Proceedings of Top Fuel 2009, pp. 2040, Paris, France, September 6-10, 2009.
- Christensen J. A., Allio R. J. and Biancheria A., *Melting point of irradiated uranium dioxide*, Transactions of the American Nuclear Society, 7(2), pp. 390-391, 1964.
- Chung H. M., Garde A. M. and Kassner T. F., *Deformation and Rupture Behaviour of Ziradol Cladding under Simulated Loss-of-Coolant Accident Conditions*, Zirconium in the Nuclear Industry, ASTM STP 633, A. L. Lowe, Jr. and G. W. Party, Eds., American Society for Testing and Materials, pp. 82-97, 1977.
- Chung H. M. and Kassner T. F., *Embrittlement Criteria for Zircaloy Fuel Cladding Applicable to Accident Situations in Light-Water Reactors*, NUREG/CR-1344, January 1980.
- Chung H. M. and Kassner T. F., *Cladding metallurgy and fracture behavior during reactivity-initiated accidents at high burnup*, Nucl. Eng. Design, 186, pp. 411-427, 1998.
- Chung H., Strain R. V, Bray T. and Billone M. C., Argonne Nat. Lab., USA, *Progress in ANL/USNRC/EPRI Program on LOCA*, Ref: Proceeding of the Topical Meeting on LOCA Fuel Safety Criteria, NEA/CSNI/R(2001)18, Aix-en-Provence, 2001.
- Chung H. M., *The Effects of Aliovalent Elements on Nodular Oxidation of Zr-Base Alloys*, Nuclear Safety Research Conference (NSRC-2003), Washington, DC, 2003.
- Chung, H. M., *Differences in Behaviour of Sn and Nb in Zirconium Metal and Zirconium Dioxide*, SEGFSM Topical Meeting on LOCA Issues Argonne National Laboratory, May 25-26, 2004.
- Clifford P., *The US Regulatory Commision's Strategy for Revising the RIA Acceptance Criteria*, Int. LWR Fuel Performance Conference, San Francisco, CA, 2007.
- Cox B., *Oxidation of Zirconium and Its Alloys*, Advances in Corrosion Science and Technology, Vol. 5, Edited by Mars G. Fontana and Roger W. Staehle, pp. 173-391, Plenum, NY, 1976.
- Cuadra A. and Diamond D. J., *BWR rod drop accident analysis*, Transactions of the American Nuclear Society, 93, pp. 376-377, 2005.
- Diamond D. J., Bromely B. P. and Aronson A., *Pulse width during a PWR rod ejection accident*, Proc: 29th Nuclear Safety Conference, Washington, DC, USA, October 2001.